IOP Conf. Series: Materials Science and Engineering **156** (2016) 012010 doi:10.1088/1757-899X/156/1/012010

Dislocation structure and deformation hardening alloy fcc single crystals at the mesolevel

L A Teplyakova[1], T S Kunitsyna[1,2], N A Koneva[1], E V Kozlov [1], A A Kondratyuk[2], N A Zboikova[1], Yu A Kakushkin[1], A A Iakhin[2]

[1]Tomsk State University of Architecture and Building, 2, Solyanaya Sq., 634003, Tomsk, Russia
[2]National Research Tomsk Polytechnic University, 30, Lenin Ave., 634050, Tomsk, Russia

E-mail: lat168@mail.ru

Abstract. The article presents the evaluation results of impacts of various strengthening mechanisms to flow stress. Such evaluations were made on the basis of the measured parameters of the dislocation substructure formed in monocrystals of [001]-Ni_3Fe alloy deformed by compression within the stage II. It was found that the main impact to deformation resistance in the alloys with net substructure is made by the mechanism of dislocation impediment, which is caused by contact interaction between moving dislocations and forest dislocations.

1. Introduction

The plastic deformation of metal materials takes place in a hierarchically organized wide interval of scales which is closely connected for the with the initial defect structure [1, 2]. As a result the scale-structural deformation level spectrum is formed. During deformation in the most well-known metal materials their multistage deformation strengthening takes place. The single-phase alloys with f.c.c. lattice, particularly monocrystals, are characterized by rather prolonged linear strengthening (stage II) which is most pronounced for the single crystals with symmetric orientations [3]. In such materials the slipping dislocations and moving point defects can be slowed down by various mechanisms and the strengthening has a complex nature. At the low temperatures the deformation is mostly provided by the dislocation movement. The analysis and systematization of all well-known strengthening mechanisms is given in [2]. At present there are about 60 of such mechanisms, 50 of them are the low temperature ones. Only this fact alone allows us to realize that to understand and describe the hierarchically organized multifactor multistage strengthening at the plastic deformation even of the materials with the f.c.c. lattice is a difficult task. It is no wonder that it is still a topical problem.

Identification of the deformation strengthening mechanisms of the metal materials requires detail data about the dislocation structure and its evolution during deformation. So since 50^{th} – 60^{th} of the XX century, the researchers have actively studied the dislocation structure of the deformed materials using the translucent electron microscopy method. Much attention was paid to the f.c.c. monocrystals, first of all to Cu, Al and Ni [4]. Studies on monocrystals let us understand the nature of the dislocation structure formation in “clean” state that is without other factors, for example such as the presence of the grain boundaries. The analysis of the deformation strengthening mechanisms should be logically carried out for the monocrystals of single phase alloy whose dislocation structure was studied in detail and the

mechanisms of its evolution in the wide interval of deformation degrees were surely confirmed. Such alloy is the Ni_3Fe alloy [3,5,6].

The given work presents the results of the experimentally determined contributions of various strengthening mechanisms realized on the first mezolevel that is the level of the dislocation substructures according to the classification considered in [2].

2. Materials and methods

In this work the Ni3Fe alloy monocrystals with the short range order were investigated. The loading axis (compression) was parallel to the crystal graphic direction [001]. The monocrystal orientations were determined using the URS – 60 apparatus by the Laue's method. The deviation from the indicated orientations in the initial state did not exceed 1 - 2°. The monocrystals had the form of the parallelepiped with the size of 3x3x6 mm3 and the side faces of the cubic orientation. The investigation of the dislocation structure was carried out on the electron microscope attached with a goniometer at the accelerating voltage of 100 and 125 kV. By the electron microscopy images of the dislocation structures the free segment lengths (λ) between various stoppers along the dislocation lines of the dislocations were measured. Such stoppers are the compound dislocation formed as the result of the dislocation reactions and the thresholds. For measuring the free segment lengths the micrographs of the foils cut parallel the octahedral plane were used. When measuring the distances between the compound dislocations no distinctions were made between the reactions in the slip plane being parallel the foil surface and the reactions with dislocations of other octahedral planes. The thresholds and bends were not distinguished. The measurements were carried out separately for the dense and thin substructure parts.

3. Results and discussion

3.1. Evolution of substructure and its spatial organiozation.

In the [001]-monocrystals of the disordered Ni_3Fe alloy the beginning of plastic deformation (transitional stage) is connected with the formation in the local monocrystal volumes of the flat dislocation clusters in the {111} planes. In the continuation of the stage II replacing it the layer net DSS is formed [6]. In the local volumes corresponding to the shift fragments with the asymmetrical slipping one system of layers with the regular-shaped net section and the increased density of dislocations parallel the primary for the given fragment of the slipping plane is formed (Figure 1). In the fragments with symmetry slipping as a rule two crossing systems of layers are formed. They are parallel each of the octahedron planes (Figure 1, near B) Rarely more than two systems of layers are formed.

3.2. Substructure hardening.

In the net substructure the deformation strength is mostly caused by the contact deceleration of moving dislocations. The following hardening mechanisms make their contribution into the contact stress (τk): 1) dislocation intersection, 2) jog dragging, 3) formation and break of deformation reactions, 4) overcoming the Lomer-Kontrell's, Hirt's dislocation barriers, etc. 5) point defect generation. The first contribution is caused by the contact interaction between the slipping and forest dislocations. Figure 2, 3 shows the histograms of the measured free segments lengths at different deformation degrees (within the stage II). As it follows from these figures the dislocation substructure (DSS) evolution is not the same in the dense and thin sections. In the thin substructure sections the λ distribution is inhomogeneous (Figure 2). The inhomogeneity is kept up to the middle of the stage II. The average length of a free segment between the reactionary junctions, jogs and any kind of these stoppers in the thin sections of the DSS is not practically decreased with the deformation degree increase (Figure.4a). Consequently, the hardening of the investigated alloy cannot be provided by the DSS thin areas. In the dense sections of DSS the λ distribution is changed with deformation (Figure 3). The maximum of the λ distribution shifts towards lower values. Within the stage II in the places with the increased density of dislocations the λ average value is decreased with the deformation increase (Figure 4b).

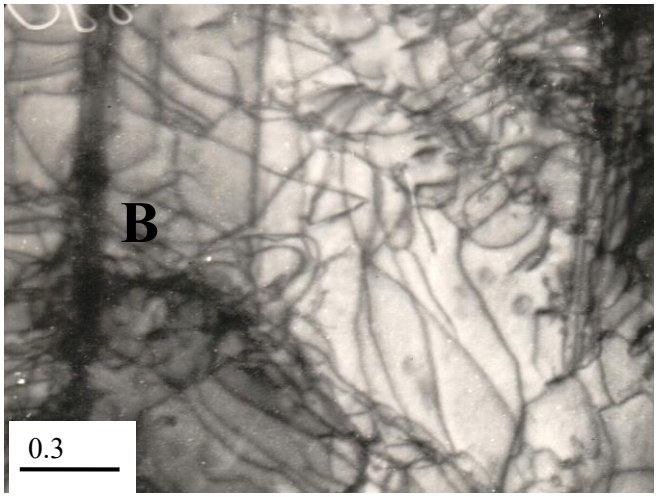

Figure 1. Dislocation structure in monocrystals Ni_3Fe, $\varepsilon = 0.17$ foil plane (111)

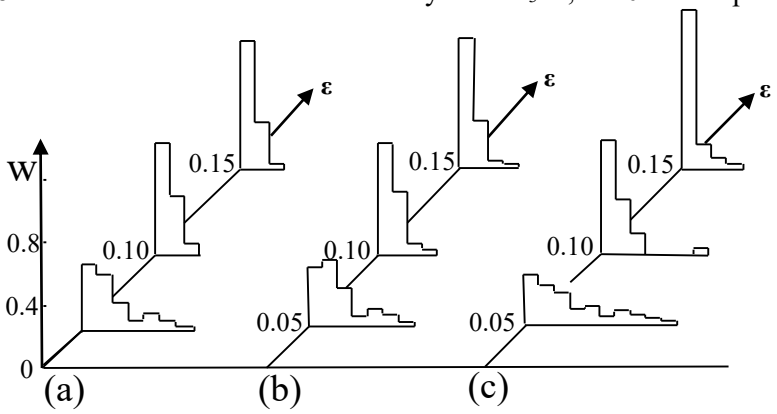

Figure 2. Histograms of the distances along the dislocation line between any stoppers (a), dislocation junctions (b), jogs (c) at various deformation degrees in the DSS dense sections.

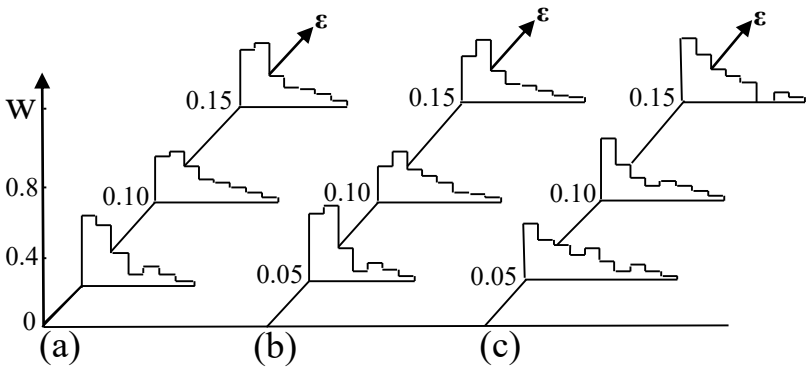

Figure 3. The same as in figure 2 but for the DSS thin sections.

Simultaneously in the crystal the volume part with the high dislocation density is increased. Slipping which is naturally developed in the weakest sections of DSS has to go through the sections with the dense net DSS due to the decrease of their quota. Thus, during deformation in the densest sections of DSS the resistance connected with the reacting forest dislocations and/or the jogs drawing will be increased.

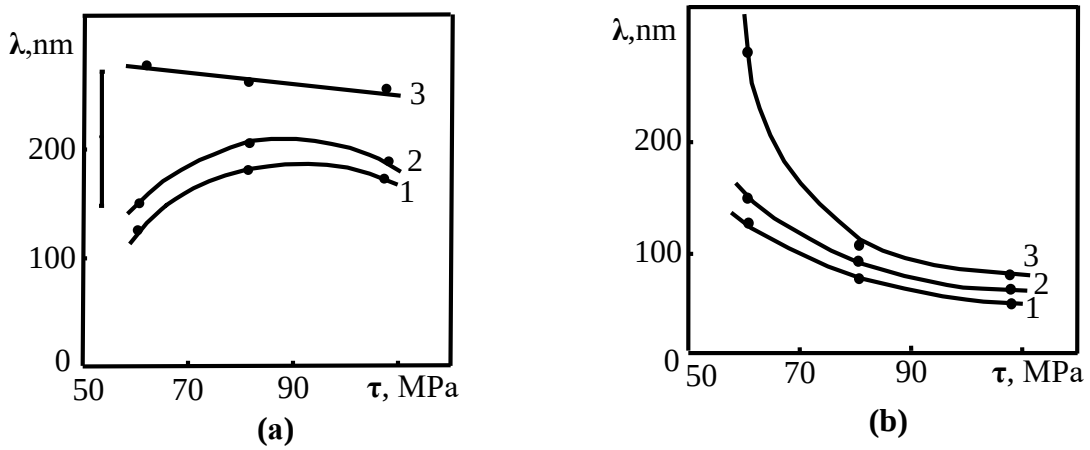

Figure 4. Dependences of the average distance along the dislocation line between any stoppers (cv.1), reactionary junctions (cv.2), jogs (cv.3) on the given stress in dense (a) and thin (b) DSS sections.

3.3. Long range order internal stress fields and elastic dislocation interaction.

The characteristic that is of primary importance in terms of the dislocation movement and multiplication is the internal stress field of the dislocation ensemble. In this paper an attempt was made to determine the magnitude (amplitude) of the long-range stress fields due to contributions from different mechanisms and determine the role of some of these mechanisms. To solve this problem the following DSS parameters were measured: 1) the bending radius of free dislocation segments; 2) the distances between the dislocations slipping both in one and in different planes; 3) the distances between the active slipping planes.

Measurement of the bending radius R let us determine the dislocation ensemble-averaged static fields of the internal stresses (IS) and their fluctuations. These fields are made up of many components: particularly, the fields from the parallel dislocations laying both in the own slipping plane and on the parallel planes; the fields formed by the forest dislocations; the fields of dislocation self-action. The values of the distances between the dislocations obtained in this work allow us to calculate the contributions to the local static field of IS. Using 3) one can determine the dynamic long-range order fields originating when the dislocations pass along the parallel planes.

3.4. Static long-range order stress fields.

The homogeneous stress τ_{st}, acting on a dislocation should bend it in an arc with a radius [7]: $R=Gb/2\tau_{st}$, where G is the shear module (for the alloy Ni_3Fe G=770 MPa), b is Burger's vector (b=0,25 μm). Here

$$\tau_{st} = \frac{Gb}{2R}$$

The bending radius is easily determined provided one knows the segment height h and the distance between the fixing points

$$R = \frac{4h^2 + l^2}{8h}.$$

Figure 5 shows the dependence of the dispersion τ_{st} on the shear stress (because the τ_{st} average value is equal to zero). As it follows from this figure the static long range order fields are significant only at the beginning of the plastic deformation. Their value is decreased with the deformation degree increase.

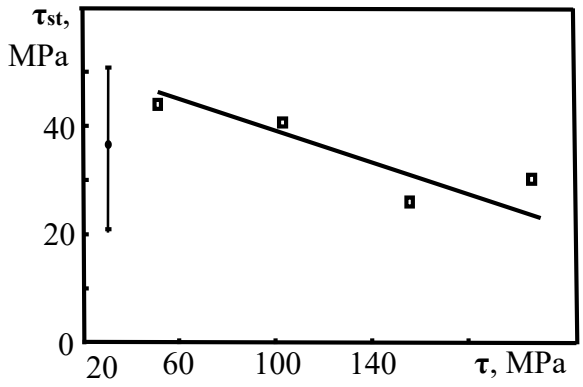

Figure 5. Dependence of the static long range order dispersion on the shear stress.

Thus the static long range order fields do not contribute to the alloy deformation strengthening (hardening). This conclusion agrees with the DSS qualitative pattern: the dislocation tangles present the multipole configurations without the excess dislocation density [2,3,5]. The free dislocation orientations along both sides the tangles are the same. This conclusion made for the high symmetrical orientation [001] where all octahedral planes are equally loaded and the secondary slipping systems are missed cannot be extended to other less symmetrical orientations without special investigation.

In the given paper the attempt was also made to single out the contribution of the elastic dislocation retardation experienced by the nearest neighboring dislocations (τs.pl) and the forest dislocations (τf)

$$\tau_{s.pl}=\frac{Gb}{2\langle L_{s.pl}\rangle};\quad \tau_f=\frac{Gb}{2\langle L_f\rangle}$$

The values of τ_{cl} and τ_f at the stage II are given in Table 1 where one sees that the elastic short-range interaction of the nearest neighbors may be significant and its role increases with the deformation. However these stresses are compensated by the elastic interaction of the second, third and the following dislocations located along the both sides of this dislocation. At full summation of the contributions of all dislocations these stresses should give zero average value and the dispersion equal to the stress of the static long-range fields.

3.5. Dynamic long-range stresses.

The resistance experienced by dislocations when passing along parallel planes can be estimated as follows:

$$\tau_{dyn}=\frac{k}{2\pi}\cdot\frac{Gb}{\langle X\rangle}$$

where < X> is the average distance between the active slipping planes; k is a factor depending on the type of dislocations that implement deformation (k=2 in case of deformation by the superdislocations, k=1 in case of the deformation by the monodislocations). The dependence of the obtained τ_{dyn} values on the deformation degree is given in Table 1. As one sees the resistance experienced by the dislocation when it moves relatively others moving along the parallel plane in the Ni_3Fe alloy is small (of the order of 30-40 MPa and remains practically unchanged at the stage II (within the spread of values)). At the beginning of the stage II τ_{dyn} may comprise a significant part of the acting stress.

Table 1. To determination of the long-range stresses

Flow stress τ (MPa)	The degree of deformation ε	Static measured average τ_{st} (MPa)	Dynamic average τ_{dyn} (MPa)	In its plane τ_{pl} (MPa)	Forests τ_f (MPa)
60	0.05	3.5	0.5	6	5.2
75	0.10		0.6	6.3	5.4
80	0.11	2.3			
90	0.15		0.7	11	9.7
105	0.17	1.5			
		By bending radius of free dislocation segments	On parallel planes for nearest traces	Elastic short-range interaction for the first neighbours	

Thus, the given evaluations of the τ_{st} and τ_{dyn} values show that in the investigated Ni_3Fe alloy with the short-range atom order the long-range fields do not play a significant role in the deformation hardening. The contact retardation (deceleration) of dislocations plays the decisive role in the hardening of this alloy (the dislocation (dislocation friction). The increase with the deformation of the stopper density along the dislocation line (both the jogs and the reactions) may be the reason of the deformation hardening. In other words, the work hardening of the Ni_3Fe disordered alloy is caused by the increase of deceleration of the dislocation friction type.

3.6. Cut dislocation density.

Measurement results of $<\lambda>$ were used to determine the $\Delta\tau_i$ contributions of the main mechanisms of the dislocation deceleration to the shear stress of the short-range atom order alloy. When determining the contributions the approximations and coefficients given in [8] were used. Table 2 presents the results of $\Delta\tau_i$ determination on the basis of the experimental $<\lambda>$ values, where где $\Delta\tau_{nc,j}$ is the resistance connected with the nonconservative jog dragging, $\Delta\tau_r$ is the resistance connected with overcoming the reacting "forest" dislocations, $\Delta\tau_d$ is the resistance connected with overcoming the long-range stress fields. Here one can see the $\Sigma\Delta\tau_i$, total values conditioned by acting of these mechanisms as well as the values of the acting shear stresses. As follows from Table 2 with the deformation degree increase the contributions caused by overcoming the resistance of reacting "forest" dislocations and jogs on the dislocations are also increased (in the DSS dense sections). At the stage II the total stress $\Sigma\Delta\tau_i$ of all mechanism contributions appears to be comparable with the stress acting in the slipping plane.

Table 2. Contributions of the main deceleration mechanisms to the shear stress.

mechanism	$\Delta\tau_{r,}$ (MPa)	$\Delta\tau_{nc.j,}$ (MPa)	$\Delta\tau_{d,}$ (MPa)	$\Sigma\Delta\tau_{i,}$ (MPa)	$\tau_{acting,}$ (MPa)
$\varepsilon = 0.05$	26	37	35	98	60
$\varepsilon = 0.10$	39	39	23	102	80
$\varepsilon = 0.15$	42	49	15	106	105

4. Conclusion

Based on the obtained results one can imagine the following scheme of the investigated alloy deformation. At the beginning of the plastic deformation when the stresses are not large only the longest free dislocation segments will take part in deformation and the dislocation slipping will occur in the less dense areas. With the increase of the stoppers density on the unit of dislocation density the longest free dislocation segments do not provide the deformation course and the slipping dislocations start cutting the areas with greater dislocation density. As a result the greater stresses should be applied for

implementation of further shear. At the same time more part of the length distribution λ is involved in the deformation. Simultaneously with the deformation degree increase the "cut" dislocation density approximates the <ρ> average value. The evaluations show that in the described scheme the dislocation slipping runs either by separation from the stoppers or by the action of free dislocation segments as the Frank-Read' sources.

References

[1] Panin V E, Grinyaev Yu V, Elsukova T F and Ivanchin A G 1982 *J. Proc. of H. Education. Phys.* **6** 5-27
[2] Kozlov E V 2002 J. Materials Questions 29 1 50 – 112
[3] Teplyakova L A, Kunitsyna T S, Koneva N A and Kozlov E V 2004 *J. Bulletin of the Russian Academy of Sciences: Physics* 68 10 1456-1461
[4] Nabarro F R N, Basinski Z S and Holt D B 1967 The Plasticity of single crystals (Moscow, Metallurgy)
[5] Koneva N A, Teplyakova L A, Kunitsyna T S and Kozlov E V 2006 Structure and properties of advanced materials (Tomck, Scientific and technical literature) p 323
[6] Teplyakova L A, Kunitsyna T S, Starenchenko V A and Poltaranin M A 2014 *J. Proc. of H. Education. Phys.* ***57*** 2 61-70
[7] Seeger A 1980 Dislocations and mechanical properties of crystals (Moscow, Publishing foreign literature)
[8] Czernikow I and Marcinkowski M I 1971 J. *Met. Trans*. **2** 3217-3222